Mechanism of strain-influenced quantum well thickness reduction in GaN/AlN short-period superlattices

2014 Nanotechnology 25 245602

(http://iopscience.iop.org/0957-4484/25/24/245602)

IOP Publishing Nanotechnology
Nanotechnology **25** (2014) 245602 (8pp) doi:10.1088/0957-4484/25/24/245602

Mechanism of strain-influenced quantum well thickness reduction in GaN/AlN short-period superlattices

A V Kuchuk[1,2], V P Kladko[1], T L Petrenko[1], V P Bryksa[1], A E Belyaev[1], Yu I Mazur[2], M E Ware[2], E A DeCuir Jr[2] and G J Salamo[2]

[1] Institute of Semiconductor Physics, National Academy of Sciences of Ukraine, Prospect Nauky 45, Kyiv 03028, Ukraine
[2] Institute for Nanoscience & Engineering, University of Arkansas, 731W. Dickson St., Fayetteville, AR 72701, USA

E-mail: ymazur@uark.edu

Received 8 February 2014, revised 3 April 2014
Accepted for publication 17 April 2014
Published 28 May 2014

Abstract
We report on the mechanism of strain-influenced quantum well (QW) thickness reduction in GaN/AlN short-period superlattices grown by plasma-assisted molecular beam epitaxy. Density functional theory was used to support the idea of a thermally activated exchange mechanism between Al adatoms and Ga surface atoms that is influenced by the strain state of the GaN QWs. These *ab initio* calculations support our experimentally observed reduction in QW thickness for different intrinsic strains.

Keywords: gallium nitride, superlattice, quantum well, strain, density functional theory

(Some figures may appear in colour only in the online journal)

1. Introduction

III-nitride nanostructures have emerged as promising materials for high-performance photonic devices operating in the infrared (IR) spectral region [1]. New intersubband (ISB) devices rely on infrared optical transitions between electronic confined states in the conduction band of GaN/Al(Ga)N superlattices (SLs). To cover the IR spectrum from the near-IR (the fiber-optic telecom wavelengths) to the far-IR (the THz spectral region, which is important for non-invasive medical diagnosis), it is enough to change only the geometrical design of SLs. Thus, ISB transitions in GaN/Al(Ga)N SLs can be tuned to the desired wavelength range by engineering the quantum well (QW) thickness.

The GaN QW thickness in such structures is normally very small (3–15 ML) due to both the large electron effective mass and the small exciton Bohr radius in GaN; small variations in the thickness of only one monolayer (1 ML = $c/2 \approx 0.26$ nm) are sufficient to lead to large changes in the ISB ($\sim$100 meV) and interband ($\sim$150 meV) transition energies for QWs of 4–5 ML [1–3]. Thus, among other factors such as defects, strain, and polarization, the optical properties of III-nitride QW devices are strongly influenced by both the quality of the interface at each layer and the precise thickness of each layer. This extreme sensitivity to fluctuations is one of the key obstacles to making optoelectronic devices based on III-nitride SLs.

Specifically, fluctuations in well widths lead to a red shift (increase in thickness) or a blue shift (decrease in thickness) of the wavelength of the main QW optical response. Both of these cases have been observed in low-temperature photoluminescence (PL) experiments [1–12]. For GaN/Al(Ga)N SLs grown by metal-organic chemical vapor deposition (MOCVD), a double PL peak structure has been observed [4, 5]. In addition to the main PL peak, the low-energy peak is explained by a discrete increase in well width of one *c*-lattice parameter (2 ML). Similar double PL peaks have been observed for SLs grown by molecular beam epitaxy (MBE) at a much lower temperature [6, 7]. It is suggested that growth interruptions at each interface both under N-rich and Ga -rich conditions lead to the discrete nature of the well width fluctuations of one (1 ML) and two (2 ML) molecular monolayers, respectively [6].

It should be noted that the growth of QW structures without interruption by using Ga as a surfactant for both GaN and AlN considerably improves their properties in terms of optical and structural characteristics [1, 3, 8, 9]. But in this case, in addition to the main QW PL peak, high-energy peaks corresponding to the well widths decreasing by one (1 ML) or two (2 ML) monolayers are observed [1, 3, 8–13]. QW thicknesses were first observed to fall short of their expected thickness for GaN/AlN SLs grown by MBE [14]. After careful growth rate calibrations, it was found that the QW thicknesses were ~30% less than expected at a growth temperature of 800 °C, whereas for 700 °C the QWs appeared to have thicknesses which were appropriately predicted by the growth rates. This reduction has been assigned to an exchange between the Ga atoms of the QW and the Al adatoms of the capping layer [15]. In this work, Gogneau *et al* studied the effect of AlN overgrowth on the structural properties of GaN nanostructures grown by plasma-assisted MBE (PAMBE) and showed that this phenomenon is thermally activated at temperatures above 720 °C. However, the mechanisms governing this exchange were not completely demonstrated.

In the current study, we report on the strain-influenced QW thickness reduction in GaN/AlN short-period SLs grown by PAMBE. The experimentally observed reduction in the GaN QW thicknesses of 1 ML and 2 ML are explained by the fact that the thermally activated exchange mechanism between the Al adatoms and the Ga surface atoms is influenced by the strain state of the GaN QWs. *Ab initio* calculations confirm our observations and improve the understanding of the microscopic mechanism of this exchange reaction.

2. Experimental results

GaN/AlN samples were grown by PAMBE on GaN buffers (0.4 μm) deposited on either GaN(5 μm)/*c*-Al_2O_3 or AlN (0.34 μm)/*c*-Al_2O_3 templates to introduce differing amounts of strain into the entire SL [16]. The active regions of the samples consisted of 30 periods of Si-doped GaN/AlN SLs with nominal thicknesses of $t_{GaN}^{nom} = 5.75 - 7.95$ ML and $t_{AlN}^{nom} = 7.95 - 8.23$ ML for the GaN and AlN layers, respectively. The samples were grown at 760 °C without interruption under an activated nitrogen plasma flux that was calibrated to grow in a nitrogen-limited regime at 0.26 ML sec^{-1}. The mass fluxes in monolayers per second (ML s^{-1}) were deduced from reflection high energy electron diffraction (RHEED) intensity oscillations at low temperature to prevent a possible underestimation due to metal desorption.

After growth, all samples were characterized by high-resolution x-ray diffraction (HRXRD) using a Philips X'pert MRD system. To understand this data, we analyzed simulated (0002) $\omega/2\,\theta$-scans using SL models where we kept the AlN thickness constant and varied the GaN thickness in increments of 1 monolayer. This is shown in figure 1(a), where we can see that these simulations are very sensitive to variations in thickness of the SL layers with better than single atomic

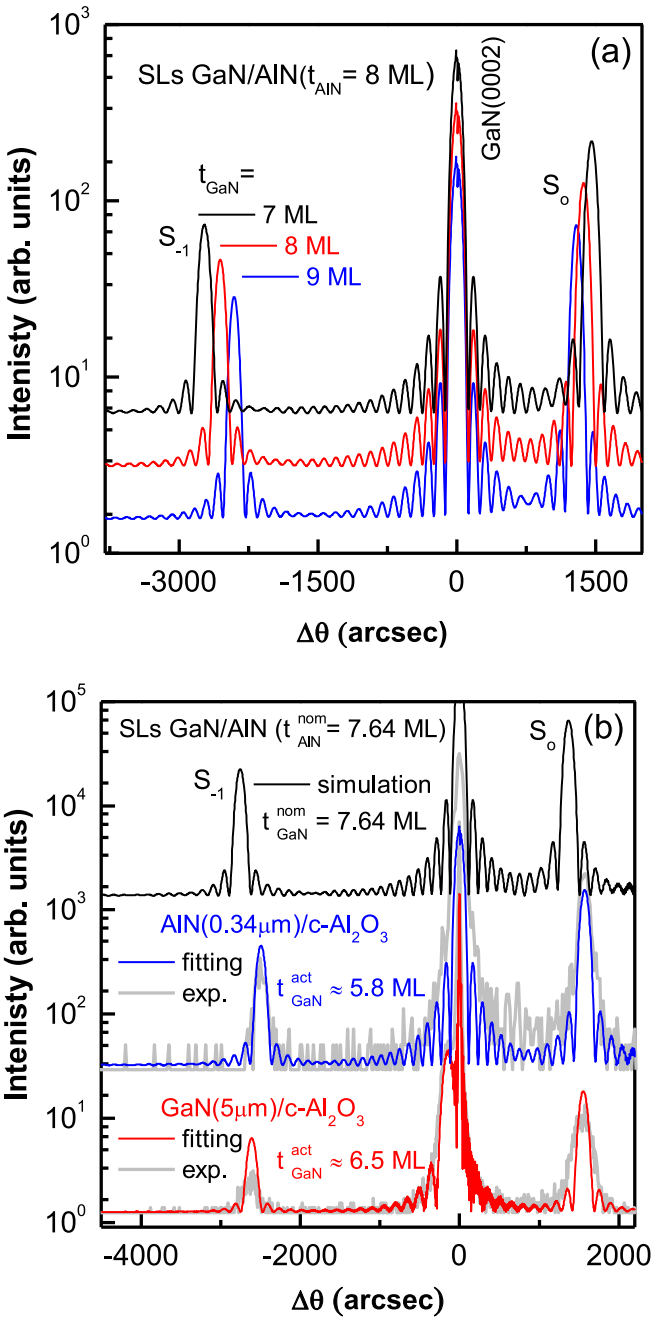

Figure 1. HRXRD (0002) $\omega/2\,\theta$ curves for GaN/AlN SLs: (a) simulated curves for $t_{GaN} = 7$, 8, 9 ML and $t_{AlN} = 8$ ML, all on a thick, relaxed GaN substrate; (b) simulated, experimental, and fitted curves for symmetrical SLs ($t_{GaN}^{nom} = t_{AlN}^{nom} = 7.64$ ML) on GaN(thick)-and AlN (thin)-on-sapphire templates.

layer characteristics. These simulations were performed using the dynamical diffraction theory and have been described in detail previously in [16]. Experimental (0002) $\omega/2\,\theta$-scans of our SL samples exhibited at least three well-resolved satellite peaks, which indicate well-defined layer periodicity with sharp interfaces. The simulated (unfitted), experimental, and fitted curves for the SLs grown on both the GaN(thick)-and AlN(thin)-on-sapphire templates are shown in figure 1(b). HRXRD rocking curve simulations confirmed that the actual

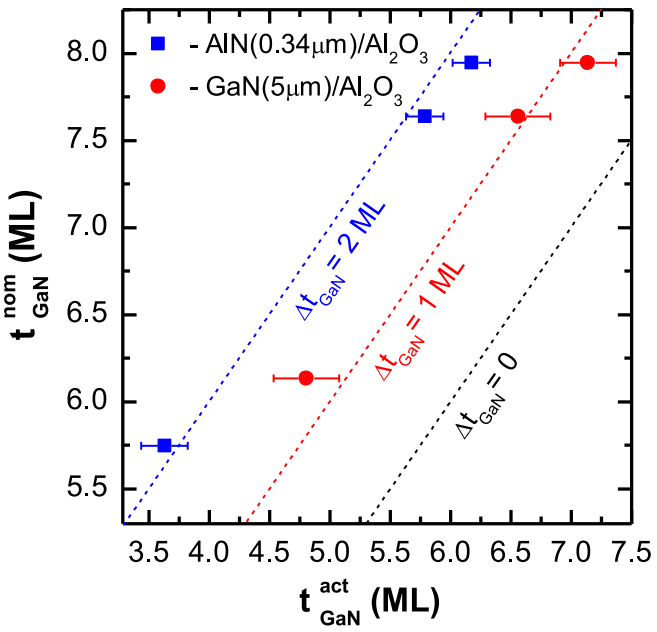

Figure 2. Nominal GaN QW thickness $\left(t_{GaN}^{nom}\right)$ versus actual GaN QW thickness $\left(t_{GaN}^{act}\right)$ for GaN/AlN SLs grown on GaN(thick)-and AlN (thin)-on-sapphire templates. The dashed lines correspond to the difference between nominal and actual GaN QW thicknesses of exactly $\Delta t_{GaN} = 0$, 1, 2 ML.

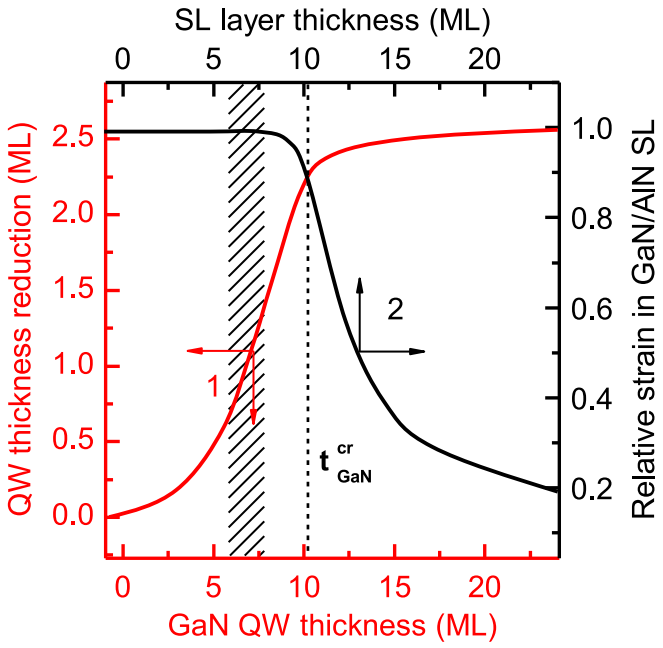

Figure 3. The red curve (1) shows the dependence of GaN QW thickness reduction on SL layer thickness from [15], and the black curve (2) shows the relative strain in asymmetric GaN/AlN SLs on the SL layer thickness from [17]. The dashed line is a guide to the eye and corresponds to the critical thickness of QW ($t_{GaN}^{cr} \sim 10$ ML). The dashed area corresponds to the GaN QWs thicknesses studied in our work.

measured thicknesses $\left(t_{GaN}^{act}\right)$ of the SL QW layers were very different from the nominal growth thicknesses $\left(t_{GaN}^{nom}\right)$ for both templates. Following [16], we used asymmetric reciprocal space maps (not shown here) to determine the deformation state of the crystal, thereby fixing the ratio of barrier to well thickness in each SL. These differences for all SL samples are summarized in figure 2. This correlates with previous results [15] because our growth temperature was above 720 °C, where the exchange between Al adatoms and the surface Ga atoms from the GaN QW was more likely. However, we show in the following paragraphs that the notably different amounts of reduction, i.e., $\Delta t_{GaN} = t_{GaN}^{nom} - t_{GaN}^{act} \approx 1$ and 2 ML, are the result of the different amounts of strain for growth on each substrate, i.e., GaN(thick)-and AlN(thin)-on-sapphire templates, respectively (see figure 2).

In addition, in [15] it was shown that GaN QW thickness has a significant effect on well thinning during the capping process. This is shown schematically by the red curve in figure 3, where the thickness reduction saturates at a critical well thickness of ~10 ML. However, the mechanism of this thinning induced by overgrowth with AlN still has not been completely explained. On the other hand, the gradual relaxation process in the GaN/AlN SL starts when the thickness of the individual layer is slightly over this critical thickness of ~10 ML, where the introduction of dislocations in the SL results in a decrease in deformation energy per layer. This has been studied in [17], from which the black curve in figure 3 is derived. Thus, as follows from figure 3, the process of thinning the GaN QWs correlates well with the process of strain relaxation in GaN/AlN SLs. Indeed, up to the critical thickness of the GaN QW ($t_{GaN} < 10$ ML), the deformation state has a strong influence on thinning. When the strain in the GaN QW starts to relax ($t_{GaN} > 10$ ML), the process of well thinning saturates.

In our previous work [18], we studied strain relaxation in GaN/AlN SL structures. It was shown that two different III-nitride substrates introduce different amounts of compensating strain into the SL layers and that pseudomorphic growth of the entire GaN/AlN SL occurs only on the AlN(thin)-on-sapphire templates. The large magnitude of mismatch in the lattice parameters makes pseudomorphic growth of SLs on GaN(thick)-on-sapphire templates impossible, and a significant density of large cracks appears on the surface. Even after this, there is a ~0.1% difference in QW residual strain on different templates. Therefore, the different residual strain in these templates induces different strain in the GaN/AlN SLs grown on them. Moreover, during the growth of the SLs on these templates, the GaN QWs are under different compressive strains, which are much more pronounced than after the growth. Taking this into account, and that the thicknesses of the GaN QWs for our samples are lower than 10 ML (see figure 3), we conclude that the degree of thickness reduction (see figure 2) is related to the different strain states in the QWs induced by the templates. In other words, the mechanism responsible for the exchange reaction between the Al adatoms and the Ga surface atoms not only is thermally activated but also depends on the deformation state of the growth surface.

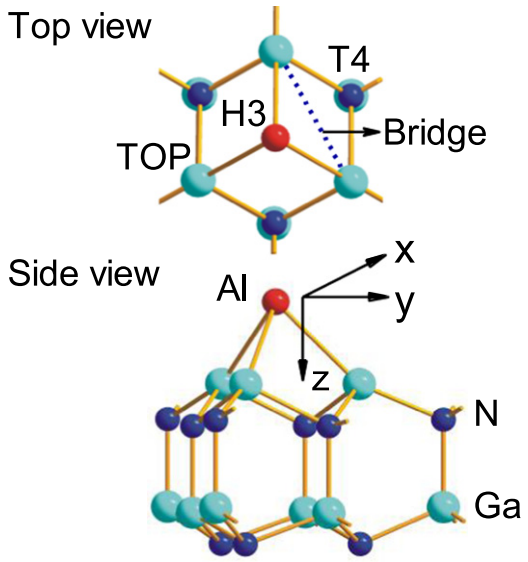

Figure 4. Top and side views of Al adatom positions on the (0001) GaN surface used for calculations. T4 and H3 positions correspond to the top of the N atom and the interstitial sites, respectively. The bridge position corresponds to a point halfway between the T4 and H3 sites.

3. The simulation procedure

For a detailed investigation of this phenomenon, we considered the Al adatom interaction with free and strained (0001) wurtzite GaN surfaces by means of density functional theory (DFT) [19]. We used a periodic (2×2) slab geometry with 4 GaN double layers and 0.9 nm of empty space between slabs. An Al adatom was placed over the Ga-terminated slab surface, while the bottom of the slab was terminated with real hydrogen atoms attached to nitrogen atoms, which in all cases were frozen in space during geometry optimization. For our calculations, we used the double-zeta plus polarization function basis (DZP) of numerical orbitals; GGA PBE functional of Perdew, Burke, and Ernzerhof [20]; the norm-conserving pseudopotentials of Troullier-Martins construction [21], which include the semicore 3D states for Ga; the $3\times3\times1$ Monkhorst-Pack grid [22]; and the finite 3D grid determined by the plane wave cutoff value equal to 300 Ry. The commonly used designations for Al adatom positions on the GaN surface that are used in the present paper are shown in figure 4.

Our use of real capped bound hydrogens in the bottom of the slab instead of pseudohydrogens with charge $Z=0.75$ requires a brief discussion. It is obvious that the perfect GaN surface is a closed-shell system that must be characterized by total spin $S=0$, while an Al adatom attached to the GaN surface is an open-shell system with total spin $S=1/2$ due to the odd number of electrons. If we use a (2×2) slab geometry with four pseudohydrogens together with an Al adatom, the total number of electrons is even. Therefore, $S=0$, and we obtain the wrong multiplicity of the system. In contrast, for a (4×4) slab geometry, which includes 16 pseudohydrogens, the total number of electrons is even, leading to an accurate value of $S=0$. Thus, to obtain the correct spin multiplicity and save computational time, we used the (2×2) slab geometry with four *real* capped bound hydrogens.

To support the validity of such an approach, we compared the total charge distributions in (2×2) supercells with real hydrogens and with pseudohydrogens, which may be characterized by Mulliken charges of atoms. Our calculations showed that only in the vicinity closest to the bottom (pseudo) hydrogen Ga and N atoms, the Mulliken charges were markedly different. At the same time, for the three upper double GaN layers, the average absolute and maximum deviations were $0.014\,e$ and $0.037\,e$, respectively. If we compare only the two upper double layers, even smaller values of $0.008\,e$ and $0.02\,e$ were obtained. Therefore, one may expect that (2×2) supercells with real capped bound hydrogens may be safely used for investigations of the interaction of an Al adatom with the GaN surface. These conclusions are in line with the results of [23], where a potential energy curve for an adatom near the GaN surface has only minor changes for pseudohydrogens with $Z=0.5$, 0.75, and 1.0 values.

4. Replacing surface Ga atoms with Al adatoms: basic mechanism and its modifications

In this section, we consider the microscopic mechanism of interaction of an Al adatom with a perfect Ga-terminated GaN (0001) surface. Such interaction determines the kinetics of the initial stage of AlN growth on GaN. We show that this process is a thermally activated one with a barrier height that is both strain and site dependent. Then we consider the influence of various factors, such as the presence of a Ga overlayer together with Al adatoms trapped in the nearest metastable positions of T4 type, on the barrier height. In addition, the energy barrier modification was calculated for the final stage of the process, when most of the surface Ga atoms were already replaced with Al. As shown in the following paragraphs, in all cases the microscopic mechanism of substituting appears to be very similar.

As a first step, we consider in detail the mechanism of substituting when an Al adatom moves toward a perfect GaN surface through the H3 position. The reaction coordinate, z, for the process of substitution of the surface Ga atom with an Al adatom was defined as follows (figure 4). With the *z*-axis perpendicular to the GaN surface, we set a z-coordinate for the Al atom and let x and y relax together with the optimization of coordinates of all slab atoms except the bottom layer of nitrogen and hydrogen, which remained fixed. Fixing the bottom layer simulates the restrictive effect of the bottom GaN double layers on the moving of atoms near the surface, substantially reducing the computation time. Through DFT, we calculated the energy variation, ΔE_{tot}, as a function of the reaction coordinate z of the Al adatom, whereas we allowed the other atomic coordinates in the slab (with the exception of the bottom layer) to relax. In all cases, the total energy

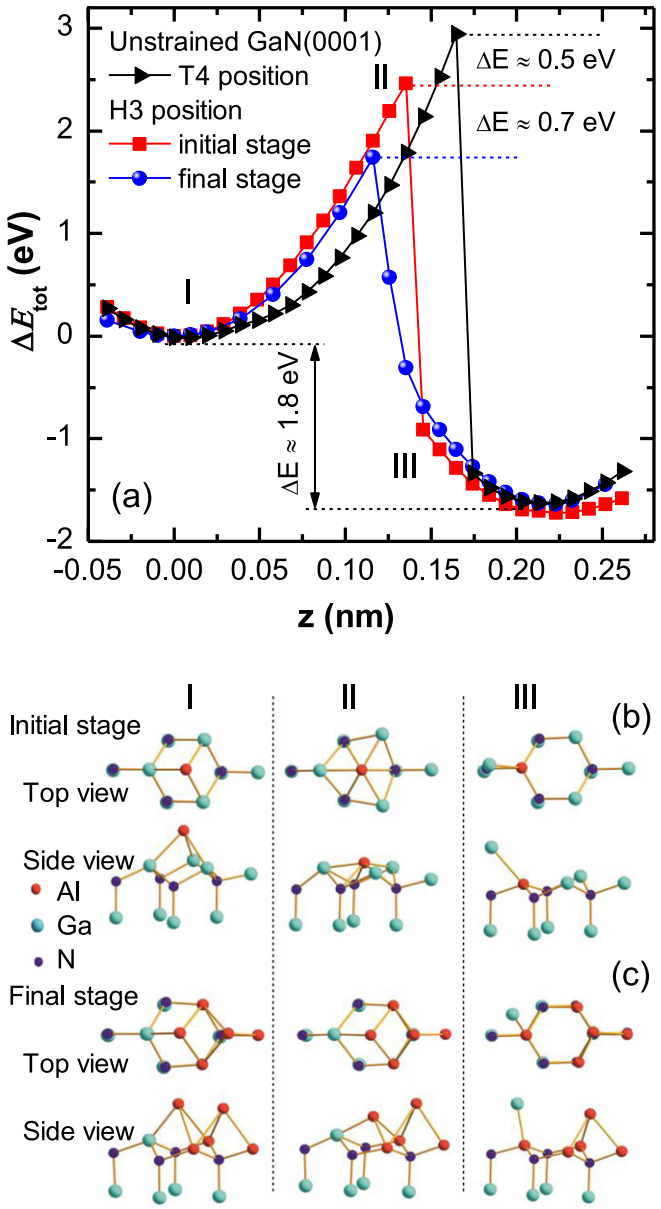

Figure 5. (a) Calculated energy barriers for replacing the Ga surface atom with an Al adatom for an unstrained GaN surface. (b) A pictorial view of the local geometry alteration when an Al adatom moves down to the GaN surface through the H3 position during the initial stages of film replacement and (c) during the final stages. In the final stage of the Al-Ga exchange process, three surface Ga atoms are already replaced by Al atoms. *I* and *III* correspond to the final stages of physisorption and chemisorption of an Al adatom, respectively, and *II* corresponds to the position where the energy barrier is the maximum for the Al-Ga exchange process.

minimum corresponding to the physisorption was taken as the defined zero.

Figure 5(a) shows these dependencies for the Al adatom initially placed in the T4 and H3 positions. One can see that both curves are of 'classical' form: points (*I*) and (*III*) correspond to final stages of physisorption and chemisorption, respectively, while point (*II*) corresponds to the barrier necessary to overcome to effect substitution of a Ga surface atom by an Al adatom. Both curves here show that the Al-Ga exchange process is exothermic (which correlates with conclusions made in [24]) and results in a considerable overall drop in energy of ~1.8 eV.

Let us consider in detail the interaction between an Al adatom in the H3 position and the GaN(0001) surface. On the microscopic level, the chemisorption process occurs in the following way (figure 5(b)). The Al adatom moves down to the surface from point (*I*) to point (*II*), causing some deformation of the GaN lattice while preserving the wurtzite structure. Then, moving down from point (*II*) to point (*III*) ($\Delta z < 0.05$ Å), the local geometry changes dramatically. As a result, the Al adatom moves laterally from H3 to the top position and incorporates into the surface lattice site, displacing the Ga atom, which moves up (≈0.2 nm over the surface) and laterally as well. Such a barrier-free sharp alteration of local geometry (SALG) mechanism is a characteristic feature of the interaction of Al with the GaN surface. When Al adatoms become sufficiently close to the surface, the SALG mechanism is 'switched on' and a sharp drop in the potential energy curve is observed.

In the final stage of the reaction (corresponding to the global energy minimum), we obtain the weakly bound Ga adatom instead of the Al, which now forms strong ionic-covalent bonds with the three nearest nitrogen atoms. Because the Al-N binding energy is much higher than the Ga-N binding energy [24, 25], the most stable configuration corresponds to the replacement of the first layer of Ga atoms by Al adatoms.

The height of the potential energy barrier is site dependent and is governed by the moment of 'switching-on' of the SALG mechanism when the Al adatom moves towards the GaN surface. As can be seen from figure 5(a), the T4 position energy barrier is 0.5 eV higher than the H3 position. As a result, when we start from the top or bridge position, the Al is shifted to H3 during total energy minimization anyway. Therefore, the interaction through the H3 position is the main channel for the replacement of a Ga surface atom with an Al adatom.

As previously considered, the SALG process corresponds to the initial stage of AlN growth, when one Al adatom interacts with a perfect Ga-terminated GaN surface. However one may expect that after replacement of some amount of surface Ga atoms by Al, the energy barrier for reaction changes. To simulate the final stages of the process of Ga-Al exchange, we consider the case when three surface Ga atoms are already substituted by Al in our supercell (see figure 5(c)). Calculations then show that in this case, the Al adatom initially placed in the H3 position falls in the metastable T4 position rather than substituting for the Ga atom. In addition, the metastable T4 positions may be directly populated, barrier-free, through the T4 position. Thus, in the final stage the nearest Al atom in the T4 position prevents the trapping of the next Al atom in the metastable state and acts as a catalyst for growth of the AlN layer. The potential energy curve corresponding to this final stage of film replacement is shown in figure 5(a). In this case, Ga-Al exchange occurs through the SALG mechanism as well and the energy barrier necessary to overcome is reduced significantly (by ~0.7 eV). According to

transition state theory, the rate constant of the Al-Ga exchange reaction is:

$$k = \frac{k_B T}{h} \exp\left(\frac{\Delta S^*}{k_B}\right) \exp\left(\frac{\Delta H^*}{k_B T}\right), \quad (1)$$

where $\Delta S^* = \Delta S^*_{config} + \Delta S^*_{vibr}$ is the variation of configuration and vibration entropies in the transition state (point *II*) as compared with the reactants, i.e., the physisorbed Al adatom and the GaN surface (point *I*) shown in figure 5; and $\Delta H^* = \Delta E_{tot} + \Delta H^*_{vibr}$ is the variation of enthalpy with ΔE_{tot} as the total energy difference equal to the barrier height obtained with our first-principle calculations. In this case, ΔS^*_{config} is exactly equal to zero, whereas vibration-related terms usually are small and the leading term determining the reaction rate is ΔE_{tot}. In this way, we estimate the increase in reaction rate in the final stage as compared with the initial stage (see figure 5) to be as large as 3.4×10^3 at a growth temperature of T = 1000 K. Therefore, our calculations predict that the initial stage of the Al adatom reaction with the GaN surface runs relatively slowly until the final stage, when the reaction rate increases sharply. This means that the overall process of Al-Ga exchange cannot be characterized by only a single value of the activation energy.

For both H3 and T4 positions, we also repeated the foregoing calculation with the introduction of biaxial compressive strain. Here the strain was introduced by reducing the equilibrium lattice constant by 1% in the lateral direction. We chose compressive strain of the QWs to match that of real GaN/AlN SLs where the GaN well is under compression and the AlN barrier is under tension. As seen in figure 6(a), for the H3 position the energy barrier is 0.25 eV higher in the case of the 1% compression as compared with the unstrained GaN (0001) surface. The T4 position shows a similar increase in the barrier height (not shown here). According to equation (1), this leads to decreasing the reaction rate up to 18 times at T = 1000 K for the compressed GaN layer as compared with the strain-free value. Thus, there is substantial influence of deformation state on the energy barrier height and on the rate of the exchange process between an Al adatom and a Ga surface atom.

It follows from these *ab initio* calculations that the energy barrier necessary to overcome for the replacement of a surface Ga atom by an Al adatom correlates well with local deformation of the GaN(0001) surface. Figure 6(b) shows that when an Al adatom is far from the surface (point *I*), the observed GaN lattice is strain free in-plane, while near point *II*, strong lateral elongation of the Ga-Ga bond occurs, induced by the presence of the Al atom. Qualitatively, the increasing energy barrier for Al-Ga exchange in GaN surfaces under compression (figure 6(a)) is caused by the increased energy cost for the surface Ga atomic displacements as the Al adatom moves down to the surface. In the case of the final stage of Ga-Al exchange shown in figure 5(c), the compressed strain increases the energy barrier as well. However, the increase in barrier energy is only 0.03 eV and is not significant in practice.

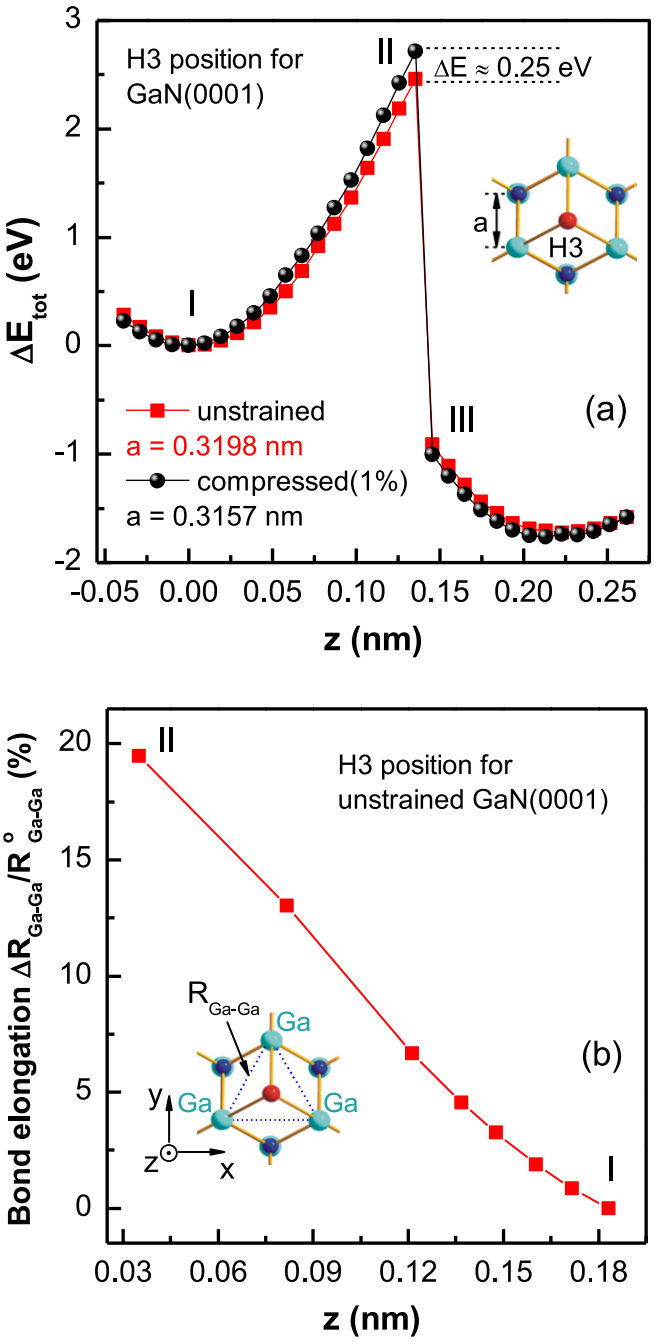

Figure 6. (a) The calculated energy barrier for replacing the Ga surface atom with an Al adatom through the H3 position for 1% biaxially compressed and unstrained GaN(0001) surfaces. (b) The dependence of the relative Ga-Ga bond elongation on the Al adatom reaction coordinate, *z*, in the H3 position for an unstrained GaN surface; $R^{o}_{Ga-Ga} = 0.317$ nm for z = 0.183 nm corresponds to the minimum *I* in figure 5(a). Notations *I*, *II*, and *III* correspond to figure 5.

It is well known that in the MBE growth of AlN/GaN quantum wells, the presence of a Ga overlayer has a strong influence on the growth rate and quality of the film. Up to 2.4 MLs of laterally contracted Ga atoms are observed experimentally, depending on the impinging Ga flux. Based on DFT calculations, the laterally contracted hexagonal

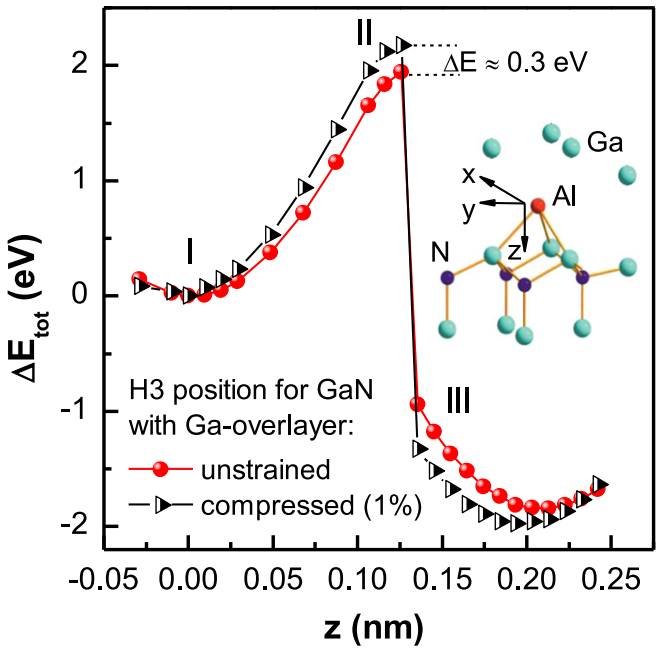

Figure 7. Calculated energy barriers for replacing the Ga surface atom with an Al adatom for unstrained and for 1% biaxially compressed GaN(0001), including a Ga overlayer. The inset illustrates the general view of the GaN(0001) surface with Al in the H3 position and the overlayer represented by Ga atoms. This optimized geometry corresponds to physisorption of an Al adatom in the presence of the overlayer.

bilayer model was suggested for the overlayer structure [26]. In the present work, we estimated the influence of such an overlayer on the energy barrier height for the Ga-Al exchange reaction. For a rough estimation of the effect, we considered the overlayer model for a GaN surface with Al adatom shown in figure 7. For the sake of simplicity, we used only one monolayer with four Ga atoms per supercell. This reproduced the experimental situation with relatively low impinging Ga flux. In addition, we fixed the lateral positions of the overlayer Ga atoms in the same positions as the surface Ga atoms, while the z-coordinates of overlayer atoms were allowed to relax. Calculations show that the SALG mechanism is still valid for the exchange reaction; however, the Ga overlayer reduces the barrier height by ~0.5 eV, which leads to a substantial increase in reaction rate of up to 3.3×10^2 times. In spite of the simplicity of this overlayer model, figure 7 supports the assumption that in the presence of a Ga overlayer, the system under consideration is sensitive to compression strains, as it is without the overlayer. However, because only a constrained geometry optimization was performed for the overlayer atoms, such a model system is not in equilibrium and we cannot make unambiguous conclusions about the quantitative influence of a Ga overlayer on the energy barrier height. This calculation only illustrates the possibility of lowering the barrier. A more rigorous simulation would deal both with sufficiently larger supercells and empty space between slabs. This is the subject of future work.

5. Discussion

As a result of the foregoing calculations, the results observed in [15, 16] concerning the QW thickness reduction for short-period GaN/AlN SLs can be explained by the fact that a thermally activated exchange mechanism between the Al adatoms and the Ga surface atoms is influenced by the strain state of the GaN QWs. *Ab initio* calculations prove that the substitution of Ga surface atoms by Al adatoms on the GaN lattice leads to a substantial reduction in energy. At the same time, the kinetics of such an exchange process depends on the GaN surface deformation state through its influence on the energy barrier height. Physically, the Al-Ga exchange requires a large displacement of the surface Ga atoms, and hence compressive strain increases the energy necessary for such large displacements.

In fact, work done in [27] has shown that strain can influence diffusion for post-growth systems as well. Here GaN QD superlattices with AlN barriers were grown. As expected, they were very stable at high temperatures, ~1150 °C. However, for very high rapid thermal anneal temperatures, >1500 °C, a preferential interdiffusion of Ga and Al was found at the apex of the QDs. It is at the apex of the QDs where the GaN lattice is largest, indicating that it is this deformation that facilitates the interdiffusion process. This is very similar to the present work in that we have demonstrated through calculations that compressive strain in the GaN layer increases the energy barrier for the exchange reaction.

Generally, GaN grown on *c*-plane sapphire is under compressive strain due to the 30° twist of the GaN unit cell with respect to the substrate *c*-axis [28]. As previously mentioned, GaN/AlN SLs naturally leave the GaN QWs under compression due to the AlN barriers. In [15], GaN/AlN SLs were grown on AlN(thick)-on-sapphire templates, resulting in a different value of the residual compressive strain; then the total strain in the GaN QWs was controlled by varying their thickness within the 2–23 ML range. Up to the critical thickness, $t_{GaN}^{cr} = 10$ ML, increasing the GaN QW thickness increases the amount of thinning up to saturation at 2 ML for $t_{GaN} \geqslant 10$ ML. This is due to the energy barrier decreasing for Al-Ga exchange as the GaN QW thickness increases because the increase in thickness reduces the total compressive strain.

In [16], varying the strain in GaN QWs while maintaining nominally the same thicknesses was achieved by growing the GaN/AlN SLs on different substrates. Growth on GaN(thick)-on-sapphire templates [18] resulted in non-pseudomorphic growth with a significant density of large cracks on the surface. Growth on AlN(thin)-on-sapphire templates [18] resulted in pseudomorphic SLs with additionally a large density of surface pits and dislocations. These results demonstrate the different compression states of the GaN QWs during the growth on each of these templates. The largest value of QW thinning (2 ML) resulted from the growth on the AlN(thin)-on-sapphire templates due to the lower

compressive strain in the GaN QWs in comparison with the QWs grown on the GaN(thick)-on-sapphire templates [18].

6. Conclusions

In this work, we have experimentally established that different amounts of residual strain from substrate lattice mismatch cause different amounts of GaN QW thickness reduction. Growth on GaN(thick)- and AlN(thin)-on-sapphire templates causes 1 and 2 ML of reduction, respectively. *Ab initio* calculations support our observations and prove that the substitution of Ga surface atoms by Al adatoms on the GaN lattice leads to a substantial lowering of the energy of the system. At the same time, the kinetics of such an exothermic exchange process depends on the GaN surface deformation state through its influence on the energy barrier height for adsorption. Physically, the Al-Ga exchange requires a large displacement of the surface Ga atoms, and hence compressive strain increases the energy necessary for such large displacements. We have demonstrated the microscopic mechanism of the exchange between Al adatoms and the Ga surface atoms in both initial and final stages of substitution. This model explains GaN QW thickness reduction during the growth of GaN/AlN SLs in terms of strain and temperature effects and must be considered for fabrication of high-quality GaN/AlN short-period SLs with controllable periods.

Acknowledgments

The authors acknowledge the financial support of the US National Science Foundation (NSF) via grant no. DMR-0520550.

References

[1] Beeler M, Trichas E and Monroy E 2013 *Semicond. Sci. Technol.* **28** 074022
[2] Machhadani H *et al* 2009 *New J. Phys.* **11** 125023
[3] Kandaswamy P K *et al* 2008 *J. Appl. Phys.* **104** 093501
[4] Haratizadeh H, Monemar B, Paskov P P, Holtz P O, Valcheva E, Persson P, Iwaya M, Kamiyama S, Amano H and Akasaki I 2007 *Phys. Status Solidi* B **244** 1727
[5] Valcheva E, Dimitrov S, Monemar B, Haratizadeh H, Persson P, Amano H and Akasaki I 2007 *Acta Phys. Pol.* A **112** 395
[6] Natali F, Cordier Y, Massies J, Vezian S, Damilano B and Leroux M 2009 *Phys. Rev.* B **79** 035328
[7] Gallart M, Lefebvre P, Morel M, Taliercio T, Gil B, Allegre J, Mathieu H, Damilano B, Grandjean N and Massies J 2001 *Phys. Stat. Sol.* A **183** 61
[8] Lahourcade L, Kandaswamy P K, Renard J, Ruterana P, Machhadani H, Tchernycheva M, Julien F H, Gayral B and Monroy E 2008 *Appl. Phys. Lett.* **93** 111906
[9] Tchernycheva M, Nevou L, Doyennette L, Julien F H, Warde E, Guillot F, Monroy E, Bellet-Amalric E, Remmele T and Albrecht M 2006 *Phys. Rev.* B **73** 125347
[10] Iizuka N, Kaneko K and Suzuki N 2002 *Appl. Phys. Lett.* **81** 1803
[11] DeCuir E A Jr, Fred E, Passmore B S, Muddasani A, Manasreh M O, Xie J, Morkoç H, Ware M E and Salamo G J 2006 *Appl. Phys. Lett.* **89** 151112
[12] Hofstetter D *et al* 2009 *J. Phys.: Condens. Matter* **21** 174208
[13] Liu X Y, Holmström P, Jänes P, Thylén L and Andersson T G 2007 *Phys. Stat. Sol.* B **244** 2892
[14] Mkhoyan K A, Silcox J, Wu H, Schaff W J and Eastman L F 2003 *Appl. Phys. Lett.* **83** 2668
[15] Gogneau N, Jalabert D, Monroy E, Sarigiannidou E, Rouviere J L, Shibata T, Tanaka M, Gerard J M and Daudin B 2004 *J. Appl. Phys.* **96** 1104
[16] Kladko V P *et al* 2011 *J. Phys. D: Appl. Phys.* **44** 025403
[17] Bykhovski A D, Gelmont B L and Shur M S 1997 *J. Appl. Phys.* **81** 6332
[18] Kladko V P, Kuchuk A V, Lytvyn P M, Yefanov O M, Safriuk N V, Belyaev A E, Mazur Yu I, DeCuir E A Jr, Ware M E and Salamo G J 2012 *Nanosc. Res. Lett.* **7** 289
[19] Soler J M, Artacho E, Gale J D, García A, Junquera J, Ordejón P and Sánchez-Portal D 2002 *J. Phys.: Condens. Matter* **14** 2745
[20] Perdew J P, Burke K and Ernzerhof M 1996 *Phys. Rev. Lett.* **77** 3865
[21] Troullier N and Martins J L 1991 *Phys. Rev.* B **43** 1993
[22] Monkhorst H J and Pack J D 1976 *Phys. Rev.* B **13** 5188
[23] Krukowski S, Kempisty P and Strak P 2013 *J. Appl. Phys.* **114** 063507
[24] Garcia-Diaz R, Cocoletzi G H and Takeuchi N 2010 *J. Cryst. Growth* **312** 2419
[25] Iliopoulos E and Moustakas T D 2002 *Appl. Phys. Lett.* **81** 295
[26] Northrup J E, Neugebauer J, Feenstra R M and Smith A R 2000 *Phys. Rev.* B **61** 9932
[27] Leclere C, Fellmann V, Bougerol C, Cooper D, Gayral B, Proietti M G, Renevier H and Daudin B 2013 *J. Appl. Phys.* **113** 034311
[28] Kladko V P, Kuchuk A V, Safryuk N V, Machulin V F, Belyaev A E, Hardtdegen H and Vitusievich S A 2009 *Appl. Phys. Lett.* **95** 031907